HOKKAIDO UNIVERSITY

Title	Fundamental peak disappears upon binding of a noble gas : a case of the vibrational spectrum of PtCO in an argon matrix
Author(s)	Ono, Yuriko; Yagi, Kiyoshi; Takayanagi, Toshiyuki; Taketsugu, Tetsuya
Citation	Physical chemistry chemical physics, 20(5), 3296-3302 https://doi.org/10.1039/c7cp06713e
Issue Date	2018-02-07
Doc URL	http://hdl.handle.net/2115/72493
Type	article (author version)
File Information	PCCP20-5 3296-3302.pdf

Instructions for use

Hokkaido University Collection of Scholarly and Academic Papers : HUSCAP

Fundamental peak disappears upon binding of noble gas: a case of vibrational spectrum of PtCO in argon matrix

Yuriko Ono,[a] Kiyoshi Yagi,[b] Toshiyuki Takayanagi,[c] and Tetsuya Taketsugu[a,*]

[a] *Department of Chemistry, Faculty of Science, Hokkaido University, Sapporo 060-0810, Japan*

[b] *Theoretical Molecular Science Laboratory, RIKEN, 2-1 Hirosawa, Wako, Saitama, 351-0198, Japan*

[c] *Department of Chemistry, Saitama University, 255 Shimo-Okubo, Sakura-ku, Saitama City, Saitama 338-8570, Japan*

ABSTRACT

Anharmonic vibrational state calculations were performed for PtCO and Ar-PtCO by the direct vibrational configuration interaction (VCI) method based on CCSD(T) energies and CCSD dipole moments at tens of thousands of grids, to get insights to anomalous effect of solid argon matrix on vibrational spectra for PtCO. It was shown that, through a binding of Ar to PtCO with a strong van der Waals interaction, the Pt-C-O bending fundamental level drastically loses the infrared intensity although the corresponding overtone band shows a relatively large intensity. The origin of this phenomenon was analyzed based on the dipole moment surfaces around the equilibrium structure. The present computations have solved the inconsistency between the gas-phase and the matrix-isolation experiments for PtCO.

* Corresponding author:
T. Taketsugu (take@sci.hokudai.ac.jp).

Introduction

Noble-gas compounds have attracted much attention last two decades. Frenking et al.[1,2] first predicted existence of neutral species containing a light noble-gas atom, Ng-BeO (Ng = He, Ne, Ar), by ab initio calculations. Later, the compounds, Ng-BeO (Ng = Ar, Kr, Xe), have been detected experimentally by Thompson and Andrews through pulsed-laser-ablation matrix-isolation spectroscopy.[3] Gerry et al. found that Ng atom makes a stable compound with a coinage metal monohalide, Ng-MX (Ng =Ar, Kr, Xe; M = Cu, Ag, Au; and X = F, Cl, Br) and determined their geometrical structures by microwave spectroscopy.[4-7] An ab initio study on these compounds showed a qualitative agreement in bond lengths with experiment.[8] There have been a few theoretical studies using highly accurate ab initio calculations for He-BeO[9-11] and He-CuF[12] for predicting spectroscopic constants of He-contained species. Ono et al. reported theoretical calculations that an argon atom possibly combines with NiCO, NiN_2, and CoCO, with a binding energy larger than a typical van der Waals interaction.[13-17] It was shown that the bending frequencies in these compounds increase by 10% due to binding with an argon atom, resulting in good agreement with the corresponding experimental frequencies recorded in solid argon. The spectroscopic constants of possible noble-gas complexes, Ng-Pd-Ng' and Ng-Pt-Ng' (Ng, Ng' = Ar, Kr, Xe), were also examined by highly accurate ab initio calculations.[18-20] Very recently, theoretical simulations were performed for experimentally observed noble-gas compounds explicitly including the matrix effects, by combining ab initio electronic structure calculations, anharmonic vibrational state calculations, and Monte Carlo simulations.[21-24]

Following theoretical predictions for Ar-NiCO,[13,16,17] we previously performed ab initio all-electron calculations for Ar-PdCO and Ar-PtCO by the QCISD(T) method with a Douglas-Kroll relativistic scheme.[25] The electronic ground states of Ar-PdCO and Ar-PtCO were predicted to be $^1\Sigma$ with linear equilibrium structures, and the binding energy with Ar was estimated as 5.3 and 8.2 kcal/mol for Ar-PdCO and Ar-PtCO, respectively. Similar to the case of Ar-NiCO, the M-C-O (M = Pd, Pt) bending frequency increases by ~10% in Ar-MCO compared to that in MCO, which is consistent with the experimental frequencies for MCO measured in the gas phase[26,27] and in solid argon matrix.[28,29] In the previous study, however, anharmonic vibrational state calculations were not carried out for Ar-PdCO and Ar-PtCO due to limitations of the computational program, and since then, there has been no theoretical study on fundamental frequencies and overtone bands, as well as on their corresponding infrared (IR) intensities, for Ar-PdCO and Ar-PtCO.

The second-order vibrational perturbation theory (VPT2)[30,31] and correlation corrected vibrational self-consistent field (cc-VSCF) methods[32,33] are widely used to compute anharmonic vibrational frequencies, which are cost-effective by treating the anharmonicity with the perturbation theory. However, floppy molecules such as Ng-MCO require a more sophisticated treatment. In particular, our interest is not only on the fundamental levels, but also on the overtones and their associated IR intensities, where the effect of anharmonicity is crucial. Vibrational configuration interaction (VCI) method based on VSCF[34,35] describes the mixing of VSCF configurations to a higher order and is more accurate. VCI method has been combined with the electronic structure calculation to compute the anharmonic potential (direct VCI method).[36] The direct VCI was previously applied to a CH_3^+ molecule to determine the rates of spontaneous emission from a CH stretching fundamental level (ν_1) to a lower energy fundamental levels, which are showing purely anharmonic effects.[37] In the present work, we use the direct VCI method to compute the vibrational frequencies and IR intensities of Ar-PtCO.

Computational details

Ab initio electronic structure calculations were carried out to determine the equilibrium structures and harmonic frequencies for the electronic ground state of PtCO and Ar-PtCO at the coupled cluster singles and doubles with a perturbational estimate of triple excitations (CCSD(T)) level, with aug-cc-pVTZ (Ar, C, O)[38,39] and aug-cc-pVTZ-PP (Pt)[40] basis sets, using the MOLPRO 2012 program package.[41,42] Subsequently, we carried out anharmonic vibrational state calculations for PtCO and Ar-PtCO using all 4 and 7 normal coordinates, respectively. (Note that both are a linear molecule with $3N - 5$ normal coordinates, where N is the number of atoms.) Fundamental frequencies, overtone, and combination bands, as well as their IR intensities, were obtained by the direct VCI methods, using the SINDO 3.6 program.[43] The calculation flow in the SINDO program is shown in a supporting information. The coupling of the potential was incorporated up to the 3rd order. CCSD(T) energies and CCSD dipole moments were calculated at the grid points used in the VSCF calculations. The number of grid points was *ca.* 4600 and *ca.* 37000 for PtCO and Ar-PtCO, respectively. The VSCF configurations employed in VCI were those excited up to 6 modes restricting the sum of quantum number to less than 6. The total number of VCI configurations was 210 and 1716 for PtCO and Ar-PtCO, respectively. To analyze dipole moment surfaces around the equilibrium structure, natural population analyses were also carried out for both PtCO and Ar-PtCO at the CCSD level with the same basis sets, using Gaussian 16.[44]

Results and discussion

Table 1 shows calculated equilibrium bond lengths and harmonic frequencies for PtCO and ArPtCO, along with available experimental data. Note that the harmonic frequencies of PtCO in gas-phase experiment are estimated values from the millimeter and submillimeter-wave spectra in the ground and excited states of Pt-C-O bending vibration,[27] while the frequencies by Ar-matrix experiment are fundamental frequencies including anharmonic effect.[29] For PtCO, the calculated harmonic frequencies are in good agreement with those in the gas phase experiment. The results for Ar-PtCO are also in good agreement with those of the Ar matrix experiment, except for the Pt-C-O bending vibrational frequency (917 cm^{-1}) is nearly double of the calculated one (461 cm^{-1}). As was already found in the previous study, the calculated frequency of the Pt-C-O bending vibration of PtCO increases from 416 to 461 cm^{-1} by about 11% in Ar-PtCO, and thus the bonding with Ar alone hardly accounts for the discrepancy.

Table 1 Calculated equilibrium bond lengths and harmonic frequencies for PtCO and Ar-PtCO at the CCSD(T) level. Experimental data are also given.

	Bond length (Å)				Harmonic frequency (cm^{-1})				
	r(Pt-C)	r(C-O)	r(Ar-Pt)		ν(CO)	ν(PtCO)	ν(PtC)	ν(ArPt)	ν(ArPtCO)
PtCO	1.766	1.153			2082	416	595		
Ar-PtCO	1.782	1.153	2.491		2084	461	586	172	69
Experimental									
Gas phase	1.760[a]	1.144[a]				420[b]	600[b]		
Ar-matrix[c]					2052	917	581		

a) Equilibrium bond lengths estimated from the rotational spectrum.[45]
b) Harmonic frequencies estimated from the rotational spectrum.[27]
c) Fundamental frequencies from Ar-matrix experiment.[29]

Table 2 shows the vibrational energy levels and IR intensities (relative intensities are given in parentheses) for the fundamental, overtone, and combination bands obtained by the direct VCI calculation for PtCO and Ar-PtCO. As to the fundamental levels, the Pt-C-O bending mode is a doubly-degenerate mode, and thus, two identical lines are given for ν(PtCO), and three energy levels are given for the Pt-C-O bending overtone states. For Ar-PtCO, vibrational states related to the modes involving

Ar motion are omitted since their intensities are negligible. As for the combination band, only the combination level of ν(CO) and ν(PtC) is given since it has a relatively large intensity. Through the comparison of harmonic frequencies in Table 1 and fundamental frequencies in Table 2, one can discuss the anharmonic effects on vibrational spectra. In Ar-PtCO, the CO stretching frequency decreases from 2084 to 2055 cm^{-1} due to the anharmonic effect (ν_{exp} = 2052 cm^{-1}), and the Pt-C stretching frequency decreases from 586 to 577 cm^{-1} (ν_{exp} = 581 cm^{-1}), both of which indicate that our calculated values are in very good agreement with the values obtained from the Ar-matrix isolation experiment. In contrast, the Pt-C-O bending frequency, which decreases from 461 to 454 cm^{-1} by considering anharmonicity, is far away from the experimental value, 917 cm^{-1}. It is notable that the overtone levels of the Pt-C-O bending vibration are lying in the range of 905 to 909 cm^{-1}, which are close to the experimental value for fundamental frequency of the Pt-C-O bending mode. As shown in Table 2, the IR intensity for the fundamental level was calculated to be 0.0001, while the IR intensity for the overtone level was calculated to be 0.0038. These results suggest that, in the Ar-matrix isolation experiment for PtCO, PtCO makes a compound with a surrounding Ar atom, resulting in generation of Ar-PtCO, and the overtone level of Pt-C-O bending vibration of Ar-PtCO was misassigned as the fundamental level of the Pt-C-O bending mode.

Table 2 Vibrational energy levels (cm^{-1}) and IR intensities (km/mol) of fundamentals, overtones, and combination bands for PtCO and Ar-PtCO calculated by the VCI method based on CCSD(T) potential energy surfaces and CCSD dipole moment surfaces. The numbers in parenthesis for the intensity are a relative value.

	PtCO			ArPtCO		
modes	$\omega(cm^{-1})$	Intensity (km/mol)		$\omega(cm^{-1})$	Intensity (km/mol)	
			Fundamentals			
ν(CO)	2052	633.4870	(1.0000)	2055	822.3970	(1.0000)
ν(PtC)	585	10.9780	(0.0173)	577	21.7701	(0.0265)
ν(PtCO)	412	2.7062	(0.0043)	454	0.0439	(0.0001)
ν(PtCO)	412	2.7062	(0.0043)	454	0.0439	(0.0001)
			Overtones			
2ν(CO)	4081	4.6703	(0.0074)	4087	4.1627	(0.0051)
2ν(PtC)	1166	0.0589	(0.0001)	1150	0.0399	(0.0000)
2ν(PtCO)	824	0.0000	(0.0000)	905	0.1538	(0.0002)
2ν(PtCO)	824	0.0000	(0.0000)	909	0.1141	(0.0001)
2ν(PtCO)	825	2.2147	(0.0035)	905	3.1408	(0.0038)
			Combinations			
ν(CO)+ ν(PtC)	2636	4.7265	(0.0075)	2631	6.4114	(0.0078)

Fig. 1 shows calculated vibrational spectra for PtCO and Ar-PtCO obtained by the direct VCI method and the experimental vibrational spectrum for PtCO by the Ar-matrix experiment. The comparison of calculated vibrational spectra for PtCO and Ar-PtCO clearly shows that the fundamental level of the Pt-C-O bending vibration loses the intensity and the overtone level is blue-shifted by about 10% upon binding with Ar. As a consequence, the calculated vibrational spectrum for Ar-PtCO is in very good agreement with the experimental one for PtCO in the Ar-matrix. This result indicates that the experimental spectrum should be ascribed to Ar-PtCO, and that the experimental peak at 917 cm^{-1}, originally assigned to the fundamental level of Pt-C-O bending vibration, should be instead assigned to the overtone level of the Pt-C-O bending vibration.

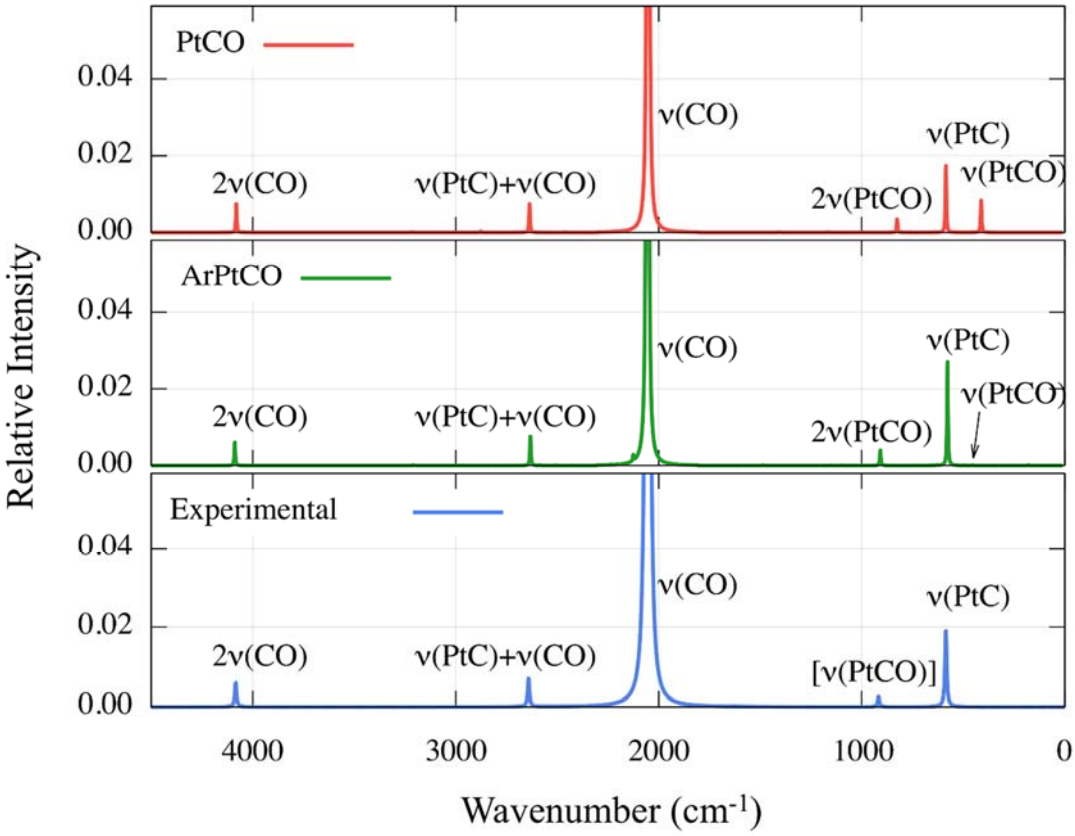

Fig. 1 The calculated IR spectra of PtCO and Ar-PtCO by the direct VCI method, and the experimental IR spectrum for PtCO in the Ar-matrix isolation. The Lorentzian function is plotted at each peak, with a half width of 5 cm^{-1}.

Hereafter, we discuss the origin of the loss of intensity of the fundamental level of the Pt-C-O bending vibration in Ar-PtCO and the relatively large intensity of the overtone level of the corresponding mode in PtCO and Ar-PtCO. Since the Pt-C-O bending vibration is a doubly-degenerate mode, there are three vibrational states related to the overtone level of Pt-C-O bending vibration for PtCO and Ar-PtCO. The calculated VCI wavefunctions are shown below:

$$\Psi_{ov1}^{PtCO} = 0.987\varphi_{0011} \quad (1)$$

$$\Psi_{ov2}^{PtCO} = 0.698\varphi_{0002} - 0.698\varphi_{0020} \quad (2)$$

$$\Psi_{ov3}^{PtCO} = 0.690\varphi_{0020} + 0.690\varphi_{0002} \quad (3)$$

$$\Psi_{ov1}^{ArPtCO} = 0.935\varphi_{0011000} \quad (4)$$

$$\Psi_{ov2}^{ArPtCO} = 0.802\varphi_{0002000} - 0.558\varphi_{0020000} \quad (5)$$

$$\Psi_{ov3}^{ArPtCO} = 0.767\varphi_{0020000} + 0.534\varphi_{0002000} \quad (6)$$

where Ψ_{ovn}^{PtCO} and Ψ_{ovn}^{ArPtCO} denote the *n*th vibrational wavefunction of the overtone levels of the Pt-C-O bending vibration for PtCO and Ar-PtCO, respectively. The VSCF

wavefunctions of PtCO and Ar-PtCO are denoted as $\varphi_{n1n2n3n4}$ and $\varphi_{n1n2n3n4n5n6n7}$, respectively, and the subscript n_i denotes a vibrational quantum number of the ith vibrational mode; the order of the vibration modes is ν(CO), ν(PtC), ν(PtCO), ν(PtCO) for PtCO and ν(CO), ν(PtC), ν(PtCO), ν(PtCO), ν(ArPt), ν(ArPtCO), ν(ArPtCO) for Ar-PtCO. In these equations, only the terms with a weight of 10% or more are given where the square of the CI coefficients is equal to the weight. The more detailed information on the CI coefficients are given in a supporting information. The order of the overtone wavefunctions corresponds to the order in Table 2 where Ψ_{ov3}^{PtCO} and Ψ_{ov3}^{ArPtCO} show a relatively large intensity. According to the CI coefficients in the above equations, the VSCF functions of the fundamental levels of stretching vibration do not contribute to the overtone levels of Pt-C-O bending vibration, indicating that Fermi resonance has no contribution to the intensity of the overtone band.

The IR absorption intensity from zero-point vibrational ground state to the nth vibrational state, B_{n0}, is given by the following equation:

$$B_{n0} = \frac{8\pi^3}{3h^2}\left[|(\mu_x)_{n0}|^2 + \left|(\mu_y)_{n0}\right|^2 + |(\mu_z)_{n0}|^2\right] \quad (7)$$

where μ_x, μ_y, and μ_z denote x, y, and z components of the dipole moment determined by the electronic wavefunction, as a function of normal coordinates. Thus, B_{n0} can be decomposed to x, y, and z-components, each of which corresponds to the square of the corresponding component of the transition dipole moment. The transition dipole moments, $(\mu_x)_{n0}$, $(\mu_y)_{n0}$, and $(\mu_z)_{n0}$, were obtained by integrating μ_x, μ_y, and μ_z with the vibrational wavefunctions over normal coordinates $\mathbf{Q}$ as,

$$(\mu_x)_{n0} = \int \Psi_n \mu_x \Psi_0 d\mathbf{Q} \quad (8)$$

$$(\mu_y)_{n0} = \int \Psi_n \mu_y \Psi_0 d\mathbf{Q} \quad (9)$$

$$(\mu_z)_{n0} = \int \Psi_n \mu_z \Psi_0 d\mathbf{Q} \quad (10)$$

In the double harmonic approximation, the dipole moment is approximated by Taylor expansion up to the first order around the equilibrium structure. In the present study, however, the dipole moments are calculated at the CCSD level at all the grid points for evaluations of the IR integrals. The use of the CCSD dipole moments around the equilibrium structure should account for the disappearance of the fundamental levels and the appearance of the overtone levels of Pt-C-O bending vibration. In other words, a higher-order polynomial term of the dipole moment (i.e., electric anharmonicity) may be the origin of the anomalous noble-gas effect on vibrational spectrum of Ar-PtCO.

As an example, in a Taylor expansion by normal coordinates $\{Q_i\}$, the *x*-component of the dipole moments is represented as,

$$\mu_x = (\mu_x)_{\mathrm{e}} + \sum_{i=1}^{3N-5} \left(\frac{\partial \mu_x}{\partial Q_i}\right)_{\mathrm{e}} Q_i + \frac{1}{2} \sum_{i,j=1}^{3N-5} \left(\frac{\partial^2 \mu_x}{\partial Q_i \partial Q_j}\right)_{\mathrm{e}} Q_i Q_j + \cdots \tag{11}$$

where a subscript "e" denotes the values at the equilibrium structure and *N* is the number of atoms included. The transition dipole moment for vibrational transition, $0 \rightarrow n$, is written as

$$(\mu_x)_{n0} = \sum_{i=1}^{3N-5} \left(\frac{\partial \mu_x}{\partial Q_i}\right)_{\mathrm{e}} \int \psi_n Q_i \psi_0 \, d\mathbf{Q} + \frac{1}{2} \sum_{i,j=1}^{3N-5} \left(\frac{\partial^2 \mu_x}{\partial Q_i \partial Q_j}\right)_{\mathrm{e}} \int \psi_n Q_i Q_j \psi_0 \, d\mathbf{Q} + \cdots \tag{12}$$

In the harmonic approximation, $\int \psi_n Q_i \psi_0 \, d\mathbf{Q}$ in the first term can have non-zero value for the fundamental level, and the electric anharmonicity terms, $\int \psi_n Q_i^2 \psi_0 \, d\mathbf{Q}$ and $\int \psi_n Q_i Q_j \psi_0 \, d\mathbf{Q}$ contribute to the overtone and combination bands, respectively. Thus, the first- and second-order derivatives of the dipole moment are the key to understand the behavior of the IR peaks.

Table 3 shows x, y, and z-components of B_{n0} in Eq. (7) for fundamentals and overtones of Pt-C-O bending vibration in PtCO and Ar-PtCO, calculated by the direct VCI method based on CCSD(T) energies and CCSD dipole moments at VSCF grid points. For both PtCO and Ar-PtCO, the molecule is located along the z-axis, and the x- and y-axes are oriented orthogonal to the molecular axis. Again, the order of overtone levels is the same as that in Table 2. As is indicated by Table 3, the transition dipole moments for the fundamentals of Pt-C-O bending vibration of PtCO decrease drastically upon binding with Ar atom, which causes disappearance of the peak of the corresponding fundamental band. It is also notable that the overtone level, $\Psi^{\mathrm{X}}_{\mathrm{ov3}}$, shows a relatively large intensity through the *z*-component of transition dipole moments, while the other levels, Ψ^{X}_{ov1} and Ψ^{X}_{ov2}, show much smaller intensity (*X* = PtCO and Ar-PtCO). The dominant term in Ψ^{X}_{ov1} is φ_{0011}, which is almost zero due to the symmetry. The dominant term in $\Psi^{\mathrm{X}}_{\mathrm{ov2}}$ is $\varphi_{0002} - \varphi_{0020}$, which is also almost zero because the contributions from φ_{0002} and φ_{0020} are cancelled each other. The dominant term in $\Psi^{\mathrm{X}}_{\mathrm{ov3}}$ is $\varphi_{0020} + \varphi_{0002}$, in which contributions from φ_{0002} and φ_{0020} are summed up, resulting in a relatively large transition dipole moment.

Table 3 The x, y, and z-components of IR absorption intensity, B_{n0} (in km/mol), for fundamentals and overtones of Pt-C-O bending vibration in PtCO and Ar-PtCO calculated by the direct VCI method.

		ω(cm^{-1})	$B_{n0,x}$	$B_{n0,y}$	$B_{n0,z}$
PtCO	ν(PtCO)	412	1.6005	1.0994	0.0000
		412	1.0994	1.6005	0.0000
	2ν(PtCO)	824	0.0000	0.0000	0.0000
		824	0.0000	0.0000	0.0000
		825	0.0000	0.0000	2.1874
Ar-PtCO	ν(PtCO)	454	0.0073	0.0364	0.0003
		454	0.0364	0.0073	0.0002
	2ν(PtCO)	905	0.0000	0.0000	0.1538
		909	0.0000	0.0000	0.1141
		905	0.0000	0.0000	3.1408

Fig. 2 shows potential energy curves and variations of the dipole moments relative to the values at the equilibrium structures, $\Delta\mu_x$, $\Delta\mu_y$, and $\Delta\mu_z$, for PtCO and Ar-PtCO as a function of Pt-C-O bending normal coordinate on the y-z plane, Q_4. The dipole moment was calculated as (μ_x, μ_y, μ_z) = (0, 0, 0.941) (PtCO) and (0, 0, 1.391) (Ar-PtCO) (in atomic unit) at the respective equilibrium structures at the CCSD level, and thus, $\Delta\mu_x$ = μ_x and $\Delta\mu_y$ = μ_y. In potential energy curves, the energy levels of the vibrational ground state (n_4 = 0; zero-point viration), the first-excited state (n_4 = 1; fundamental), and the second-excited state (n_4 = 2; overtone) are also denoted by lines. In the overtone level, the vibrational wavefunction spreads in a region of Q_4 = -50 ~ 50 bohr emu$^{1/2}$. Under the double harmoic approximation, μ_x, μ_y, and μ_z are approximated as a linear function. Due to symmetry, μ_x keeps zero value. μ_y is a linear function, but the gradient for Ar-PtCO becomes much smaller than the gradient for PtCO, leading to drastic decrease in transition dipole moment of the fundamental level of Pt-C-O bending vibration for Ar-PtCO. Therefore, the origin for disappearance of the fundamental level of Pt-C-O bending

vibration is not the electric anharmonicity effect, but the change of a linear dipole moment upon binding of Ar atom. Due to symmetry, $\Delta\mu_z$ is an even function, so it keeps a zero value under the linear approximation. As shown in Fig. 2, however, the second-order derivative of $\Delta\mu_z$ gives a relatively large value in a range of fundamental and overtone vibrational states, leading to a relatively large transition dipole moment of the overtone band of Pt-C-O bending vibration for both PtCO and Ar-PtCO.

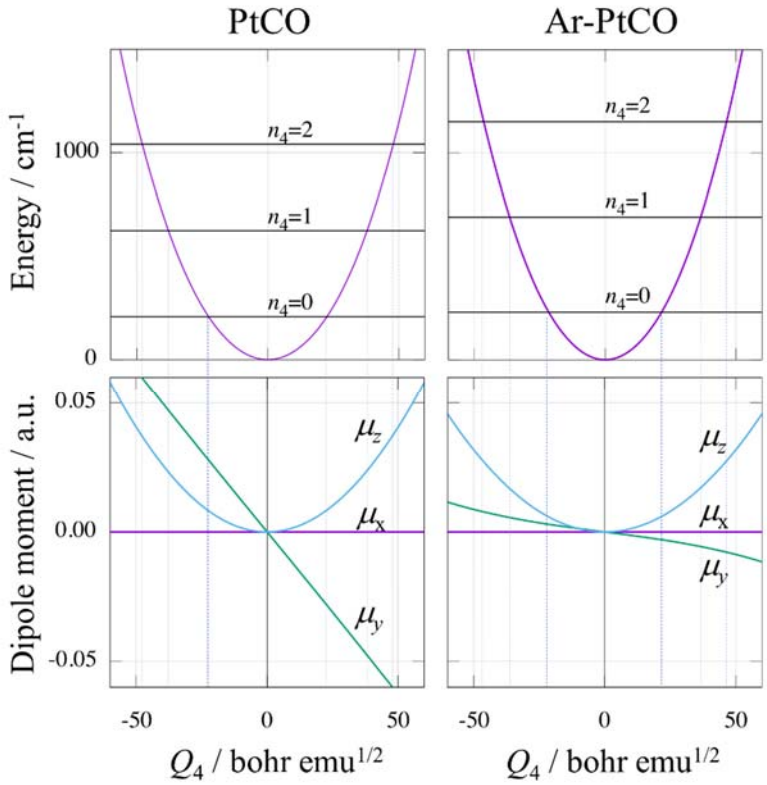

Fig. 2 Potential energy curves and variations of dipole moments of PtCO and Ar-PtCO, as a function of the Pt-C-O bending normal coordinate, Q_4.

To get further insights to the origin of a drastic change in a variation of μ_y along the Q_4 coordinate in Ar-PtCO, we investigated the atomic natural charge and electron density ($\rho(x, y, z)$) at the CCSD level. In the Pt-C-O bending overtone level, the vibrational wavefunction spreads in a range of Q_4 = -50 ~ 50 bohr emu$^{1/2}$, and so we examined atomic charges at the VSCF grid point closest to the classical turning point of Pt-C-O bending overtone level (Q_4 = 46.5 bohr emu$^{1/2}$ for PtCO and Q_4 = 44.2 bohr emu$^{1/2}$ for Ar-PtCO). At the equilibrium structure, atomic natural charges were calculated to be -0.093 (Pt), 0.557 (C), and -0.464 (O) for PtCO, while the corresponding charges were -0.199 (Pt), 0.556 (C), -0.468 (O), and 0.110 (Ar) for Ar-PtCO, indicating that 0.1

electron is transferred from Ar to PtCO. At the bent structure, atomic charges were calculated to be -0.072 (Pt), 0.541 (C), and -0.469 (O) for PtCO, while the corresponding charges were -0.181 (Pt), 0.543 (C), -0.471 (O), and 0.108 (Ar) for Ar-PtCO. Thus, in both molecules, a small amount of electron is transferred from Pt to the other atoms through Pt-C-O bending motion. **Figs. 3a** and **3b** show the contour maps of the electron density difference $\Delta\rho = \rho(\text{Ar-PtCO}) - (\rho(\text{Ar}) + \rho(\text{PtCO}))$ at the equilibrium linear geometry ($\Delta\rho_{\text{linear}}$) and at the bent geometry with Q_4 = 44.2 bohr emu$^{1/2}$ ($\Delta\rho_{\text{bent}}$), respectively, on the y-z plane at the CCSD level where the position of each atom for ρ(Ar) and ρ(PtCO) is determined to coincide with that for ρ(Ar-PtCO). Blue color denotes an increase of the electron density, while red color denotes a decrease of the electron density. Fig. 3a shows a tendency of electron transfer from Ar to Pt, which is also supported by the change of atomic natural charges mentioned above. At the bent structure in Fig. 3b, Ar and Pt are located almost on the z-axis due to relatively heavy masses, and only C and O atoms move largely in y-direction, generating a dipole moment in the y-direction from O atom (negative charge) to C atom (positive charge). It is noted that, in Fig. 3b, the largest change in the electron density is observed around the Pt atom. **Fig. 3c** shows the contour map of the difference of the electron density difference, $\Delta\rho_{\text{bent}} - \Delta\rho_{\text{linear}}$. This figure clearly shows that, due to the existence of Ar atom, electron transfer occurs from right to left especially at Pt and C atoms, which works to cancel the dipole moment of μ_{CO} in the y-direction. Such a change of the electron density in Ar-PtCO is the origin of disappearance of the fundamental level of Pt-C-O bending vibration. It can be concluded that Ar atom brings anomolous effects on both the Pt-C-O bending frequency (10% increase) and the absorption intensity (disappearance of fudnamental peak).

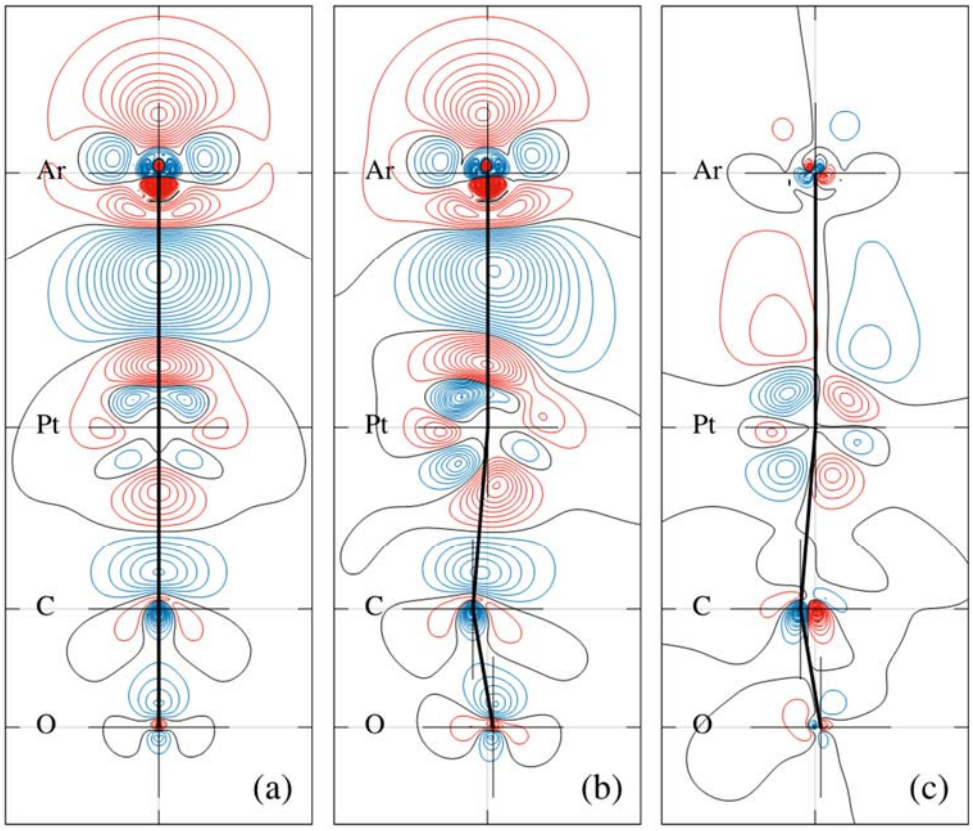

Fig. 3 The contour maps of the electron density difference $\Delta\rho = \rho(\text{Ar-PtCO}) - (\rho(\text{Ar}) + \rho(\text{PtCO}))$ (a) at the equilibrium linear geometry (referred to as $\Delta\rho_{\text{linear}}$) and (b) at the bent geometry with $Q_4 = 44.2$ bohr emu$^{1/2}$ (referred to as $\Delta\rho_{\text{bent}}$), on the y-z plane at the CCSD level; (c) the contour map of the difference of the electron density difference $\Delta\rho_{\text{bent}} - \Delta\rho_{\text{linear}}$. Blue color denotes an increase of the electron density, while red color denotes a decrease of the electron density. The contour interval is 0.001.

Concluding remarks

In this study, we investigated anomalous noble gas effects on PtCO by calculating the IR vibrational spectra for PtCO and Ar-PtCO, with referring the IR vibrational spectra of PtCO measured in the Ar-matrix isolation experiment. The vibrational frequencies (fundamental frequencies, overtone, and combination bands) and the corresponding IR intensities were calculated using the direct VCI methods based on the CCSD(T) energies and CCSD dipole moments at tens of thousands of the grid points around the equilibrium structures, using the SINDO 3.6 program. It was shown that Ar is bound to PtCO with a strong van der Waals interaction, and the Pt-C-O bending frequency increases by *ca.* 10%. The VCI calculations indicate that the IR intensity for the fundamental level of the Pt-C-O bending vibration becomes almost negligible in Ar-PtCO, resulting in a disappearance of the Pt-C-O bending fundamental level in the IR spectrum. On the other hand, the overtone level for the Pt-C-O bending vibrations shows a relatively large intensity, suggesting a misassignment of the Pt-C-O bending fundamental level of PtCO in Ar-matix. The origin of this anomalous intensity for the Pt-C-O bending mode was ascribed to a drastic change in variations of the dipole moment along the Pt-C-O bending normal coordinates in Ar-PtCO. This finding was clearly explained by showing the electron density difference for ρ(Ar) + ρ(PtCO) → ρ(Ar-PtCO) at linear and bent structures.

Conflicts of interest

The authors declare no competing financial interest.

Acknowledgments

This work was supported by JSPS KAKENHI with Grant Number 16KT0047 (to Taketsugu) and JP16H00857 (to Yagi), and partly supported by MEXT as "Priority Issue on Post-K computer" (Development of new fundamental technologies for high-efficiency energy creation, conversion/storage and use). Y. O. would like to thank E. Y. Okabayashi and T. Okabayashi for fruitful discussions and valuable suggestions. A part of calculations was performed using the Research Center for Computational Science, Okazaki, Japan.

Notes and references

1 W. Koch, J. R. Collins, and G. Frenking, *Chem. Phys. Lett.*, 1986, **132**, 330.

2 G. Frenking, W. Koch, J. Gauss, and D. Cremer, *J. Am. Chem. Soc.*, 1988, **110**, 8007.

3 C. A. Thompson and L. Andrews, *J. Am. Chem. Soc.*, 1994, **116**, 423.

4 C. J. Evans and M. C. L. Gerry, *J. Chem. Phys.*, 2000, **112**, 1321.

5 C. J. Evans and M. C. L. Gerry, *J. Chem. Phys.*, 2000, **112**, 9363.

6 J. M. Thomas, N. R. Walker, S. A. Cooke, and M. C. L. Gerry, *J. Am. Chem. Soc.*, 2004, **126**, 1235.

7 S. A. Cooke and M. C. L. Gerry, *J. Am. Chem. Soc.*, 2004, **126**, 17000.

8 C. Lovallo and M. Klobukowski, *Chem. Phys. Lett.*, 2003, **368**, 589.

9 T. Takayanagi, H. Motegi, Y. Taketsugu, and T. Taketsugu, *Chem. Phys. Lett.*, 2008, **454**, 1.

10 H. Motegi, A. Kakizaki, T. Takayanagi, Y. Taketsugu, T. Taketsugu, and M. Shiga, *Chem. Phys.*, 2008, **354**, 38.

11 M. Hapka, J. K□os, T. Korona, and G. Cha□asi□ski, *J. Phys. Chem. A*, 2013, **117**, 6657

12 T. Tanaka, T. Takayanagi, T. Taketsugu, and Y. Ono, *Chem. Phys. Lett.*, 2012, **539-540**, 15.

13 Y. Ono and T. Taketsugu, *Chem. Phys. Lett.*, 2004, **385**, 85.

14 Y. Ono and T. Taketsugu, *J. Chem. Phys.*, 2004, **120**, 6035.

15 Y. Ono and T. Taketsugu, *J. Phys. Chem. A*, 2004, **108**, 5464.

16 Y. Ono and T. Taketsugu, *Monatsch. Chem.*, 2005, **136**, 1087.

17 Y. Taketsugu, T. Noro, and T. Taketsugu, *J. Phys. Chem. A*, 2008, **112**, 1018.

18 J.V. Burda, N. Runeberg, and P. Pyykkö, *Chem. Phys. Lett.*, 1998, **288**, 635.

19 Y. Ono, T. Taketsugu, and T. Noro, *J. Chem. Phys.*, 2005, **123**, 204321.

20 Y. Taketsugu, T. Taketsugu, and T. Noro, *J. Chem. Phys.*, 2006, **125**, 154308.

21 A. Nakayama, K. Niimi, Y. Ono, and T. Taketsugu, *J. Chem. Phys.*, 2012, **136**, 054506.

22 K. Niimi, A. Nakayama, Y. Ono, and T. Taketsugu, *J. Phys. Chem. A*, 2014, **118**, 380.

23 K. Niimi, T. Taketsugu, and A. Nakayama, *Phys. Chem. Chem. Phys.*, 2015, **17**, 7872.

24 C. Zhu, K. Niimi, T. Taketsugu, M. Tsuge, A. Nakayama, and L. Khriachtchev, *J. Chem. Phys.*, 2015, **142**, 054305.

25 Y. Taketsugu, T. Noro, and T. Taketsugu, *Chem. Phys. Lett.*, 2010, **484**, 139.

26 T. Okabayashi, T. Yamamoto, E. Y. Okabayashi, and M. Tanimoto, *J. Phys. Chem. A*, 2011, **115**, 1869.

27 E. Yamazaki, T. Okabayashi, M. Tanimoto, *Chem. Phys. Lett.*, 2004, **396**, 150.

28 B. Tremblay, L. Manceron, *Chem. Phys.*, 1999, **250**, 187.

29 L. Manceron, B. Tremblay, M.E. Alikhani, *J. Phys. Chem. A*, 2000, **104**, 3750.

30 V. Barone, *J. Chem. Phys.*, 2004, **122**, 014108.

31 J. Bloino, M. Biczysko, and V. Barone, *J. Chem. Theory Comput.*, 2012, **8**, 1015.

32 L. S. Norris, M. A. Ratner, A. E. Roitberg, and R. B. Gerber, *J. Chem. Phys.*, 1996, **105**, 11261.

33 G. M. Chaban and R. B. Gerber, *J. Chem. Phys.*, 2001, **115**, 1340.

34 S. Carter, S. J. Culik, and J. M. Bowman, *J. Chem. Phys.*, 1997, **107**, 10458.

35 J. M. Bowman, T. Carrington, and H.-D. Meyer, *Mol. Phys.*, 2008, **106**, 2145.

36 K. Yagi, T. Taketsugu, K. Hirao, and M. S. Gordon, *J. Chem. Phys.*, 2000, **113**, 1005.

37 R. D. Thomas, I. Kashperka, E. Vigren, W. Geppert, M. Hamberg, M. Larsson, M. af Ugglas, V. Zhaunerchyk, N. Indriolo, K. Yagi, S. Hirata, and B. J. McCall, *Astrophys. J.*, 2012, **758**, 55.

38 T.H. Dunning, Jr. *J. Chem. Phys.*, 1989, **90**, 1007.

39 D.E. Woon and T.H. Dunning, Jr. *J. Chem. Phys.*, 1993, **98**, 1358.

40 D. Figgen, K.A. Peterson, M. Dolg, and H. Stoll, *J. Chem. Phys.*, 2009, **130**, 164108.

41 H.-J. Werner, P. J. Knowles, G. Knizia, F. R. Manby and M. Schütz, *WIREs Comput. Mol. Sci.*, 2012, **2**, 242.

42 MOLPRO, version 2012.1, a package of ab initio programs, H.-J. Werner, P. J. Knowles, G. Knizia, F. R. Manby, M. Schütz, P. Celani, T. Korona, R. Lindh, A. Mitrushenkov, G. Rauhut, K. R. Shamasundar, T. B. Adler, R. D. Amos, A. Bernhardsson, A. Berning, D. L. Cooper, M. J. O. Deegan, A. J. Dobbyn, F. Eckert, E. Goll, C. Hampel, A. Hesselmann, G. Hetzer, T. Hrenar, G. Jansen, C. Köppl, Y. Liu, A. W. Lloyd, R. A. Mata, A. J. May, S. J. McNicholas, W. Meyer, M. E. Mura, A. Nicklass, D. P. O'Neill, P. Palmieri, D. Peng, K. Pflüger, R. Pitzer, M. Reiher, T. Shiozaki, H. Stoll, A. J. Stone, R. Tarroni, T. Thorsteinsson, and M. Wang, see http://www.molpro.net.

43 SINDO 3.6: A suite of programs including a potential energy surface - dipole moment surface generator and solver of the vibrational many-body problem developed by K. Yagi (2017).

44 Gaussian 16, Revision A.03, Frisch, M. J.; Trucks, G. W.; Schlegel, H. B.; Scuseria, G. E.; Robb, M. A.; Cheeseman, J. R.; Scalmani, G.; Barone, V.; Petersson, G. A.;

Nakatsuji, H.; Li, X.; Caricato, M.; Marenich, A. V.; Bloino, J.; Janesko, B. G.; Gomperts, R.; Mennucci, B.; Hratchian, H. P.; Ortiz, J. V.; Izmaylov, A. F.; Sonnenberg, J. L.; Williams-Young, D.; Ding, F.; Lipparini, F.; Egidi, F.; Goings, J.; Peng, B.; Petrone, A.; Henderson, T.; Ranasinghe, D.; Zakrzewski, V. G.; Gao, J.; Rega, N.; Zheng, G.; Liang, W.; Hada, M.; Ehara, M.; Toyota, K.; Fukuda, R.; Hasegawa, J.; Ishida, M.; Nakajima, T.; Honda, Y.; Kitao, O.; Nakai, H.; Vreven, T.; Throssell, K.; Montgomery, J. A., Jr.; Peralta, J. E.; Ogliaro, F.; Bearpark, M. J.; Heyd, J. J.; Brothers, E. N.; Kudin, K. N.; Staroverov, V. N.; Keith, T. A.; Kobayashi, R.; Normand, J.; Raghavachari, K.; Rendell, A. P.; Burant, J. C.; Iyengar, S. S.; Tomasi, J.; Cossi, M.; Millam, J. M.; Klene, M.; Adamo, C.; Cammi, R.; Ochterski, J. W.; Martin, R. L.; Morokuma, K.; Farkas, O.; Foresman, J. B.; Fox, D. J. Gaussian, Inc., Wallingford CT, 2016.

45 C. J. Evans and M. C. L. Gerry, *J. Phys. Chem. A*, 2001, **105**, 9659.